

Slow down of the electronic relaxation close to the Mott transition

Sharareh Sayyad^{1,2} and Martin Eckstein^{1,2}

¹Max Planck Institute for the Structure and Dynamics of Matter, 22761 Hamburg, Germany

²University of Hamburg-CFEL, 22761 Hamburg, Germany

(Dated: January 13, 2016)

We investigate the time-dependent reformation of the quasiparticle peak in a correlated metal near the Mott transition, after the system is quenched into a hot electron state and equilibrates with an environment which is colder than the Fermi-liquid crossover temperature. Close to the transition, we identify a purely electronic bottleneck timescale, which depends on the spectral weight around the Fermi energy in the bad metallic phase in a non-linear way. This timescale can be orders of magnitude larger than the bare electronic hopping time, so that a separation electronic and lattice timescales may break down. The results are obtained using nonequilibrium dynamical mean-field theory and a slave-rotor representation of the Anderson impurity model.

PACS numbers: 71.10.Fd

When the Mott metal-insulator transition [1] is approached from the metallic side, a narrow quasi-particle band emerges at the Fermi energy, and spectral weight is transferred into the Hubbard bands. This behavior, which is observed in a large class of materials, is a paradigm manifestation of many-body correlations, and its theoretical description has been a major success of dynamical mean-field theory (DMFT) [2, 3]. By means of photo-excitation, metallic phases in Mott insulators can be induced on femtosecond timescales [4–6], which provides an intriguing example for ultra-fast switching material properties. While it is well understood that an intense laser pulse can rapidly promote electrons to effective temperatures of several $1000K$ and thus lead to a partial melting of the Mott gap [5], the equilibrium properties of such a high-temperature state would correspond to a bad metal rather than a Fermi liquid [7, 8]. It thus remains a fundamental question, with immediate importance for understanding the transport properties of photo-excited metallic states, how fast coherent quasi-particles can be formed as the excitation energy is passed from the electrons to the lattice.

Naively one may expect that the electrons in a metal thermalize to a quasi-equilibrium state almost instantly after the excitation, and quasiparticles are formed as soon as the effective temperature is low enough. The relevant timescale for this process would then be set by the electron-lattice relaxation. However, while rapid thermalization can be understood within a quasiparticle picture (from a kinetic equation), the latter provides no clue about the timescale for the evolution of the density of states itself, as long as quasiparticles are not yet well-defined. Considerable progress in describing the dynamics of Mott insulators has been made using nonequilibrium DMFT [9], but a study of the correlated metal close to the Mott transition has remained elusive. Although the quasiparticle peak within DMFT corresponds to the Kondo resonance in an effective impurity model [2], its formation in time can be expected to show an entirely dif-

ferent dynamical behavior that the classic problem of the buildup of Kondo screening [13–18], because the spectral weight responsible for the Kondo screening is formed *self-consistently* in DMFT. Impurity solvers such as higher-order strong-coupling expansions [10], Monte Carlo [11], or density-matrix renormalization group [12] have not yet reached sufficiently long times in this parameter regime.

In equilibrium, the slave-rotor approach developed by Florens and Georges [19, 20] provides an intuitive semi-analytical understanding of the Mott transition, by representing electrons in terms of a quantum rotor (charge) and a spinful fermion. In this paper we solve the coupled spinor and rotor equations out of equilibrium, and show that the two partial degrees of freedom become almost decoupled during the evolution. As a consequence, bad metallic behavior prevails in a photo-excited state over times which can be orders of magnitude longer than the electron hopping, and therefore even become comparable to the electron-phonon relaxation time.

Model: We study the particle-hole symmetric Hubbard model

$$H = -J \sum_{\langle ij \rangle, \sigma} (c_{i\sigma}^\dagger c_{j\sigma} + h.c.) + U \sum_i (n_{i\uparrow} - \frac{1}{2})(n_{i\downarrow} - \frac{1}{2}), \quad (1)$$

where J is the hopping amplitude (which will be time-dependent), U is the on-site Coulomb repulsion, $c_{i\sigma}$ and $c_{i\sigma}^\dagger$ are electron annihilation and creation operators for spin $\sigma \in \{\uparrow, \downarrow\}$ on site i , and $n_{i\sigma} = c_{i\sigma}^\dagger c_{i\sigma}$. The model is solved within nonequilibrium DMFT [9] on a Bethe lattice, i.e., it is mapped onto an Anderson impurity problem with self-consistently determined hybridization function $\Delta(t, t') = J(t)G_{loc}(t, t')J(t')$ [2], where $G_{loc}(t, t') = -i\langle T_C c(t)c^\dagger(t') \rangle$ is the local contour-ordered Green's function [21].

To solve the nonequilibrium dynamics of this model, we employ the $U(1)$ slave-rotor representation [19]. The impurity operators $(c_\sigma, c_\sigma^\dagger)$ are substituted by $c_\sigma^\dagger = f_\sigma^\dagger e^{i\theta}$, where f_σ^\dagger is a fermion and $\theta \in [0, 2\pi)$ is a quantum rotor variable. A constraint $L = \sum_\sigma f_\sigma^\dagger f_\sigma - 1$ on the angu-

lar momentum $L = i\partial_\theta$ of the rotor removes unphysical states from the Hilbert space. With this, the interaction Hamiltonian is determined only by the rotor, $H_U = UL^2/2$, while f_σ represents a charge-less fermion (spinon). Furthermore, the rotor is replaced by a bosonic field $X = e^{i\theta}$ with the constraint $|X(t)|^2 = 1$. The dynamics of the Anderson model is then analyzed in terms of contour-ordered rotor and spinon Green's functions

$$G_X(t, t') = -i\langle T_C X(t) X^*(t') \rangle, \quad (2a)$$

$$G_f(t, t') = -i\langle T_C f_\sigma(t) f_\sigma^*(t') \rangle, \quad (2b)$$

where G_X has a direct relation to the local charge susceptibility [19]. The model can be solved exactly when the spin-degeneracy N and the number of rotor flavors M is increased from $N = 2$ and $M = 1$ to infinity, keeping the ratio $\mathcal{N} = N/M$ fixed [19], and this limit provides a qualitatively correct description of the metal-insulator transition. (Below we fix the parameter $\mathcal{N} = 3$, for which the DMFT phase-diagram is quantitatively reproduced [19].) The derivation of the resulting integral equations for G_X and G_f in real time is a straightforward reformulation of the original work [19] on the Keldysh contour, and we just state the final result: The Green's functions (2) satisfy Dyson equations

$$(i\partial_t - \mu)G_f(t, t') - [\Sigma_f * G_f](t, t') = \delta_C(t, t'), \quad (3)$$

$$\left(\frac{-1}{4U}\partial_t^2 + \eta\right)G_X(t, t') - [\Sigma_X * G_X](t, t') = \delta_C(t, t'), \quad (4)$$

where $\Sigma_X(t, t') = i\mathcal{N}\Delta(t, t')G_f(t', t)$ and $\Sigma_f(t, t') = i\Delta(t, t')G_X(t', t)$, are rotor and spinor self-energies. The time-dependent Lagrange multiplier $\eta(t)$ must be determined such that the constraint $|X(t)|^2 = 1$ is satisfied. The electron's Green's function is obtained by $G_{loc}(t, t') = iG_f(t, t')G_X(t, t')$, closing the equations with the DMFT self-consistency. Equations (3) and (4) are solved using the Volterra integral techniques described in Ref. [9], and $\eta(t)$ is determined by a predictor-corrector procedure.

Results: In Fig. 1a, we plot the electronic density of states for three temperatures at $U/J = 4$. (The metal insulator transition endpoint is at $U_c \approx 4.69J$). Below a temperature $T^* \approx 0.2J$, a quasiparticle peak emerges at the Fermi energy, while for $T > T^*$ the system is in a bad metallic state with a pseudo-gap at the Fermi energy. To study the time-dependent formation of quasiparticles, we initially prepare the system in the atomic limit ($J = 0$), and rapidly turn on the hopping to a value $J_* > 0$. (In the following, J_* and \hbar/J_* set the energy and time unit, respectively, and the ramp-on profile is given by $J(t) = J_*(1 - \cos(\pi t/t_c))/2$ for $0 \leq t \leq t_c = 2.5$.) At intermediate values of U and in an isolated system, such a quench would lead to a highly excited electronic state which thermalizes within few $1/J_*$ to an effective temperature above the Fermi-liquid crossover T_* [22], which is also confirmed by the slave-rotor calculations. Hence this

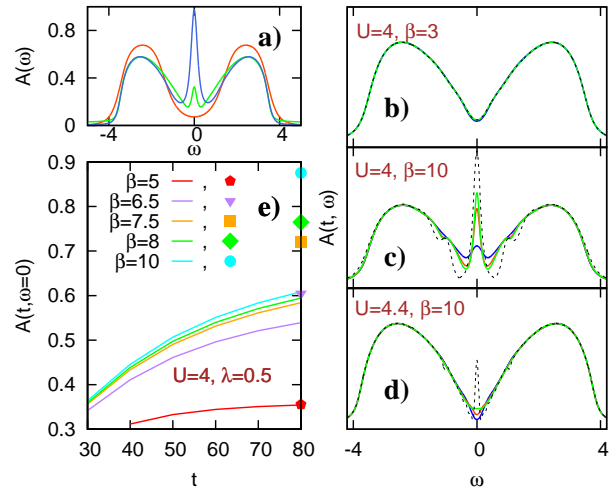


FIG. 1. a) Equilibrium density of state $A(\omega)$ for three different temperatures $\beta = 1$ (red), $\beta = 5$ (green) and $\beta = 7$ (blue) throughout the metal-insulator crossover at $U = 4$. b-d) $A(\omega)$ in equilibrium (dashed line) compared to the time-dependent spectral function $A(t, \omega)$ for $\lambda = 0.5$ at times $t = 20$ (blue), $t = 50$ (red), and $t = 80$ (green) and values of U and β as indicated. e) The height of the quasiparticle peak $A(t, \omega = 0)$ as a function of time for $U = 4$, bath temperatures $\beta = 5, 6.5, 7.5, 8, 10$ (from bottom to top) and bath coupling $\lambda = 0.5$. Symbols on the right vertical axis correspond to the equilibrium value $A(\omega = 0)$ at the same temperatures.

excited state is a good representation of a hot-electron state reached after strong photo-excitation. In addition, the system is weakly coupled to a bosonic heat bath at low temperature $T = 1/\beta$, to cool down the electrons and form the Fermi liquid when U/J_* is in the metallic phase. We treat this dissipative bath by an additional electron self-energy $\Sigma_{bath}(t, t') = \lambda D(t, t')G(t, t')$, where D is the noninteracting bosonic Green's function with frequency ω_0 , set to $\omega_0 = 1$, and λ is the coupling constant [23].

To track the time-evolution of the system, we compute the time-dependent spectral functions $A(t, \omega) = -\frac{1}{\pi} \text{Im} \int_0^t ds G^{\text{ret}}(t, t-s) e^{i\omega s}$. For bath temperatures $T > T^*$, $A(\omega, t)$ is almost indistinguishable from the equilibrium spectrum $A(\omega)$ at temperature T already at early times $t = 20$ (Fig. 1b). For lower temperature, however, only the Hubbard bands are rapidly retrieved, while the formation of the quasiparticle peak remains incomplete even for times larger than the inverse width of the peak (Fig. 1c). The closer U is to the critical value U_c , the less metallic is the transient state (Fig. 1d). The slow evolution is also clear from the time-evolution of the spectral weight $A(t, \omega = 0)$ (Fig. 1e): For $T < T^*$, the equilibrium value $A(0)$ strongly increases with decreasing T , while the time-dependent value $A(t, 0)$ becomes almost independent of the bath temperature, indicating that the dynamics is governed by a bottleneck of electronic nature.

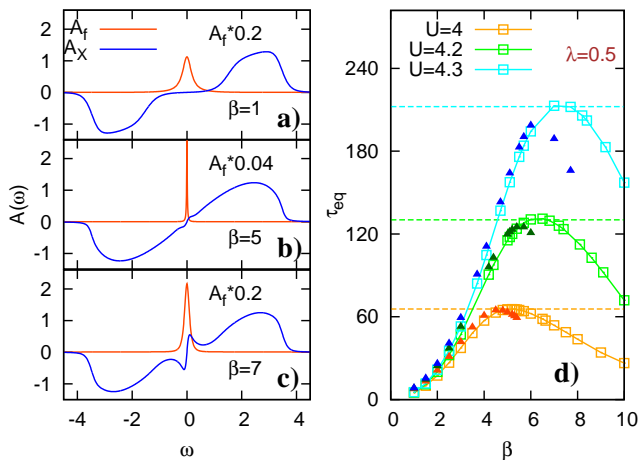


FIG. 2. a-c) Spinon (f) and rotor (X) spectral functions in equilibrium for $U = 4$ and temperatures in the bad metal regime ($\beta = 1$, a), the crossover ($\beta = 5$, b) and the metallic phase ($\beta = 7$, c). d) The spinon lifetime (inverse width of the peak) as a function of β for different values of U . Triangular points are calculated using the approximate expression Eq.(6). Dashed lines indicate the maximum spinon lifetime τ_{\max} during the relaxation process (see main text and Fig. 3).

In order to understand this behavior, we first analyze it in terms of the rotor and spinon degrees of freedom. Despite the well-known equilibrium physics of the Hubbard model, the slave-rotor language exhibits a nontrivial spinon response in the crossover regime. Figure 2a-c shows the spectral functions $A_{X,f}(\omega) = -\frac{1}{\pi} \text{Im} \int ds G_{X,f}^{\text{ret}}(s) e^{i\omega s}$ in equilibrium. At high-temperature, the rotor has spectral weight around the Hubbard bands, and the spinon peak is broadened due to the interaction with the charge fluctuations (Fig. 2a). Below the crossover (Fig. 2c), the rotor develops low-energy spectral weight, which implies the formation of the quasi-particle peak [19]. In the intermediate temperature regime, however, spinon and rotor become energetically decoupled, and $A_f(\omega)$ develops into a narrow Lorentzian peak (Fig. 2b). The width Γ of the Lorentzian defines a timescale $\tau_{\text{eq}}(T) = 1/\Gamma$, which has a clear maximum τ_* as a function of temperature in the metal-insulator crossover (Fig. 2d). To characterize the time evolution, we plot $G_f^{\text{ret}}(t, t-s)$ as a function of time difference s for various t (Fig. 3). A narrow peak in $A_f(\omega)$ corresponds to a slow decay of G_f as a function of s , so that we can define a nonequilibrium spinon lifetime by

$$\tau_{\text{ne}}^{-1}(t) = -\partial_s G_f^{\text{ret}}(t, t-s) / G_f^{\text{ret}}(t, t-s)|_{s=s_0} \quad (5)$$

for some fixed time s_0 . (For a Lorentzian peak, τ is the inverse width). The time τ_{ne} first increases with t and then decreases, tracking the evolution of $\tau_{\text{eq}}(T)$ a function of temperature (Fig. 3b). We then find that the maximum of $\tau_{\text{ne}}(t)$ as a function of time (τ_{\max}) coincides with the crossover scale τ_* (dashed lines in Fig. 2d), and

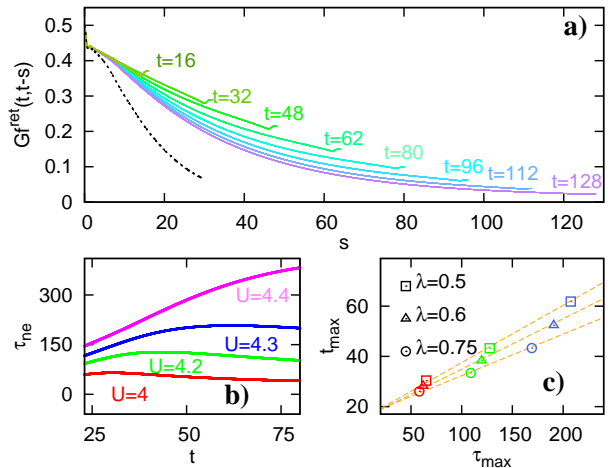


FIG. 3. a) Retarded spinon Green's function $G_f^{\text{ret}}(t, t-s)$ as a function of relative time s for various different times t ($U = 4$, $\beta = 10$, $\lambda = 0.5$), and in equilibrium (dashed line). The slope decreases for $t \lesssim 32$ and increases for $t \gtrsim 32$. b) Inverse of the slope [Eq. (5)] as a function of t for $\lambda = 0.5$, $\beta = 10$, $s_0 = 16$ and various values U below the metal-insulator transition. c) Crossover time t_{\max} plotted against τ_{\max} , where (t_{\max}, τ_{\max}) corresponds to the maximum of the curves $\tau_{\text{ne}}(t)$ in panel b).

moreover, this value is reached at a time t_{\max} proportional to τ_* (Fig. 3c). This demonstrates that the long lifetime of the spinon provides a bottleneck time for he relaxation in the crossover regime.

Although properties of $A_f(\omega)$ are not simply reflected in the equilibrium single-particle properties, one can approximately express the timescale τ_* in terms of the electronic degrees of freedom. The width of a sharp resonance in $A_f(\omega)$ is given by the imaginary part of the self-energy Σ_f , which depends on G_X and Δ . In the crossover regime, we can, to a first approximation, relate the rotor G_X to the electronic Green's function by $A(\omega) = \frac{1}{2} A_X''(\omega) \coth(\beta\omega/2)$, by setting $A_f(\omega) = \delta(\omega)$ in the convolution $G_{\text{loc}}(t, t') = iG_f(t, t')G_X(t, t')$ [24]. Analytic continuation of $\Sigma_f(t, t') = i\Delta(t, t')G_X(t', t)$ then gives

$$\tau_{\text{eq}}^{-1}(T) = -\Sigma_f''(\omega = 0) \approx -\int d\omega \frac{\Delta''(\omega)A(\omega)}{\cosh(\omega/2T)^2}, \quad (6)$$

and $\tau_* = \tau_{\text{eq}}(T_*)$, which agrees well with the numerical result (Fig. 2d). For the Bethe lattice $\Delta = J^2 G_{\text{loc}}$, so that $\Delta''(\omega) = -\pi J^2 A(\omega)$. Equation (6) implies a rather nontrivial relation between the nonequilibrium relaxation and the electronic properties. At T_* , the hyperbolic cosine function restricts the integral to values close to the pseudo-gap, where $A(\omega)$ is small. Since the endpoint of the metal-insulator transition temperature in the Hubbard model is remarkably small compared to the bare energy scales, τ_* becomes much longer than the bare hopping close to the transition $U = U_c$.

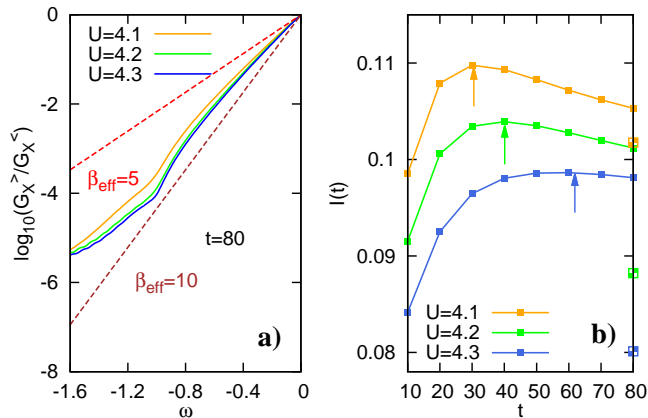


FIG. 4. Test of the quasi-equilibrium relation $G_X^>(\omega, t)/G_X^<(\omega, t) = e^{\beta_{\text{eff}}\omega}$ at $t = 80$ for $U = 4, 4.2, 4.3$ ($\lambda = 0.75$, $\beta = 10$). b) Integrated spectral weight $I(t) = \int_0^{0.5} d\omega A_X(t, \omega)$ of the rotor at low energy. Square half-filled points at $t = 80$ correspond to the equilibrium values. Arrows indicate the t_{max} (Fig. 3c).

To further analyze the relaxation, we investigate whether rotor reaches a quasi-equilibrium state while the spinon is slowly evolving. One can check this by testing the fluctuation-dissipation $G_X^>(\omega, t)/G_X^<(\omega, t) = e^{\beta_{\text{eff}}\omega}$ is satisfied, which would imply that an effective temperature $T_{\text{eff}} = 1/\beta_{\text{eff}}$ can be assigned to charge fluctuations (using the time-dependent Fourier transforms $G^{>,<}(\omega, t) = \int ds G^{>,<}(t, t-s)e^{i\omega s}$). Figure 4a however shows that a single charge temperature cannot be defined on the timescale of the simulation. While the occupation of high-energy fluctuations (the Hubbard bands) is small, the low energy part, which is more strongly influenced by the nonequilibrium spinor, remains at an apparent higher temperature, i.e., high-energy and low-energy charge fluctuations are not thermalized with each other. Because of the coupling between the spinon and the rotor, the low-energy spectral weight of the rotor also reflects the non-monotonous evolution of the spinor (Fig. 4b): The increase of the spinon bandwidth for $t > t_{\text{max}}$ leads to the transfer of rotor spectral weight to higher energies, so that the integrated spectral weight of the rotor in the low energy region $0 < \omega < 0.5$ has a maximum around $t = t_{\text{max}}$.

Conclusion and Discussion: In conclusion, we have investigated how the electronic state close to the Mott transition in the Hubbard model relaxes from an excited hot-electron state towards the Fermi liquid. We found a bottleneck time of purely electronic nature, before which charge and electronic degrees of freedom remain in a non-thermal state and cannot be characterized by an effective temperature, and the formation of the quasiparticle band is incomplete. The electronic relaxation is related to the spinon lifetime τ_* , and a simple estimate [Eq. (6)] in terms of the density of states around $\omega = 0$ at the

crossover temperature T_* (the onset of quasiparticle formation) shows that this time can be much longer than the femtosecond hopping time. The absence of quasiparticles implies long-lived bad metallic behavior, and should thus be observable also in optical experiments on materials like LiV_2O_4 , which are metals close to the paramagnetic Mott transition [25, 26]. We note that slow (or absent) formation of a quasiparticle band was also observed in simulations of a photo-doped Mott-insulator [23], but in this case the origin of the behavior is less clear because the final low temperature state is insulating.

It is important to note that the τ_* characterizes the slow dynamics of the system around the crossover regime, but not necessarily the subsequent reshaping of the quasiparticle peak. Times larger than t_{max} cannot be studied systematically due to the increase of the numerical cost with the simulated time. This prevents a systematic study of the final formation of the quasiparticle peak, which might bring in another slow timescale related to the build-up of low energy spectral weight of the rotor. Furthermore, after quasiparticles are formed, slow dynamics can arise also from an ineffective coupling of heavy electrons to phonons [27].

The observed dynamical behavior arises from the DMFT self-consistency and is thus a lattice effect, entirely different from the build-up of the Kondo peak after a quench in the Anderson model, which is limited only by energy-time uncertainty [13]. A natural question for future studies is thus whether a similar electronic bottleneck time may appear in multi-band Hubbard models or the Kondo lattice model for heavy fermions, where localized f or d orbitals interacting with delocalized electrons giving rise to the emergence of massive quasiparticles. In this context it is also interesting whether one can identify the small energy scale related to the spinon in numerically exact equilibrium calculations.

The authors would like to acknowledge fruitful discussions with A. Rosch, D. Golez, and Ph. Werner.

-
- [1] M. Imada, A. Fujimori, and Y. Tokura, Rev. Mod. Phys. **70**, 1039 (1998).
 - [2] A. Georges, G. Kotliar, W. Krauth, and M. J. Rozenberg, Rev. Mod. Phys. **68**, 13 (1996).
 - [3] G. Kotliar, S. Y. Savrasov, K. Haule, V. S. Oudovenko, O. Parcollet, and C. A. Marianetti, Rev. Mod. Phys. **78**, 865 (2006).
 - [4] S. Iwai, M. Ono, A. Maeda, H. Matsuzaki, H. Kishida, H. Okamoto, and Y. Tokura, Phys. Rev. Lett. **91**, 057401 (2003).
 - [5] L. Perfetti, P. A. Loukakos, M. Lisowski, U. Bovensiepen, H. Berger, S. Biermann, P. S. Cornaglia, A. Georges, and M. Wolf, Phys. Rev. Lett. **97**, 067402 (2006).
 - [6] D. Wegkamp, M. Herzog, L. Xian, M. Gatti, P. Cudazzo, C. L. McGahan, R. E. Marvel, R. F. Haglund, A. Rubio, M. Wolf, and J. Stähler, Phys. Rev. Lett. **113**, 216401 (2005).

- (2014).
- [7] J. Merino and R. H. McKenzie, *Phys. Rev. B* **61**, 7996 (2000).
- [8] X. Deng, J. Mravlje, R. Žitko, M. Ferrero, G. Kotliar, and A. Georges, *Phys. Rev. Lett.* **110**, 086401 (2013).
- [9] H. Aoki, N. Tsuji, M. Eckstein, M. Kollar, T. Oka, and Ph. Werner, *Rev. Mod. Phys.* **86**, 779 (2014).
- [10] M. Eckstein and Ph. Werner, *Phys. Rev. B* **82**, 115115 (2010).
- [11] Ph. Werner, T. Oka, and A. J. Millis, *Phys. Rev. B* **79**, 035320 (2009).
- [12] F. A. Wolf, I. P. McCulloch, and U. Schollwöck, *Phys. Rev. B* **90**, 235131 (2014).
- [13] P. Nordlander, M. Pustilnik, Y. Meir, N. S. Wingreen, and D. C. Langreth, *Phys. Rev. Lett.* **83**, 808 (1999).
- [14] F. B. Andres and A. Schiller, *Phys. Rev. Lett.* **95**, 196801 (2005).
- [15] D. Roosen, M. R. Wegewijs, and W. Hofstetter, *Phys. Rev. Lett.* **100**, 087201 (2008).
- [16] G. Cohen, E. Gull, D. R. Reichman, A. J. Millis, and E. Rabani, *Phys. Rev. B* **87**, 195108 (2013).
- [17] G. Cohen, E. Gull, D. R. Reichman, and A. J. Millis, *Phys. Rev. Lett.* **112**, 146802 (2014).
- [18] A. E. Antipov, Q. Dong, E. Gull, arXiv:1508.06633 (2015).
- [19] S. Florens and A. Georges, *Phys. Rev. B* **66**, 165111 (2002).
- [20] S. Florens and A. Georges, *Phys. Rev. B* **70**, 035114 (2004).
- [21] For an introduction and notation concerning nonequilibrium Green's functions, see Ref. [9].
- [22] M. Eckstein and Ph. Werner, *Phys. Rev. B* **84**, 035122 (2011).
- [23] M. Eckstein and Ph. Werner, *Phys. Rev. Lett.* **110**, 126401 (2013).
- [24] For the analytic continuation of the slave-rotor equations to the real-frequency axis, see Ref. [19].
- [25] J. Matsuno, K Kobayashi, A Fujimori, L.F Mattheiss, Y Ueda, *Physica B* **28**, 281-282 (2000).
- [26] R. Arita, K. Held, A. V. Lukoyanov, and V. I. Anisimov, *Phys. Rev. Lett.* **98**, 166402 (2007).
- [27] J. Demsar, R. D. Averitt, K. H. Ahn, M. J. Graf, S. A. Trugman, V. V. Kabanov, J. L. Sarrao, and A. J. Taylor, *Phys. Rev. Lett.* **91**, 027401 (2003).